

Progress in effective field theory approach to the binary inspiral problem

Ira Z. Rothstein

Received: 1 March 2014 / Accepted: 31 March 2014 / Published online: 8 May 2014
© Springer Science+Business Media New York 2014

Abstract In this article I review the progress made in understanding the binary in spiral problem using Effective Field Theory technology.

Keywords Effective field theory · Gravity waves

1 Introduction

General Relativity (GR) is, almost by definition, a theory of geometry. The equations of motion follow from varying an action whose form is uniquely fixed by general coordinate invariance.¹ However, in the middle of the last century an alternate, though of not logically distinct, approach was instigated in which the Einstein equations were derived starting from the assumption of massless spin two particle in a flat background. These ideas were pioneered by Gupta [1] and Kraichnan [2], and independently by Feynman [3]. In the latter case it was clear that the motivation arose from a desire to quantize gravity in analogy with Yang-Mills theory. Indeed 50 years ago at this very conference in Warsaw, Feynman presented his results on the subject. Later Weinberg [4] gave a very elegant proof of the need for the graviton to couple to a conserved current, at linearized level, and the accompanying (strong) equivalence principle by assuming that quantum mechanical amplitudes involving (soft) graviton emission should obey the standard assumptions of unitarity and analyticity in quantum field theory. In this methodology the structure of GR stems from the mismatch between number of degrees

¹ This talk is only concerned with classical relativity.

This article belongs to the Topical Collection: The First Century of General Relativity: GR20/Amaldi10.

I. Z. Rothstein (✉)
Department of Physics, Carnegie Mellon University, 15213 Pittsburgh, PA, USA
e-mail: izr@andrew.cmu.edu

of freedom represented by on-shell asymptotic states (two transverse helicities) and the symmetric two index Lorentz tensor field. In particular, the diffeomorphism invariance is necessary in order to be able to eliminate the unphysical degrees of freedom that are forced upon us by the Lorentz group.

This non-geometric² (quantum based) approach does have the added benefit that one can utilize the machinery developed for quantum field theory, including Feynman diagrams, to organize calculations. Indeed, in Duff [5] the Schwarzschild solution was generated by coupling the graviton a point particle classical source and calculating all the tree level diagrams which contribute to the expectation value of the metric. The solution is then built up order by order in G_N . Whether or not the full solution (including the horizon) emerges by summing the series (i.e. whether or not the series is asymptotic) is unknown. This question is complicated by the fact that this calculation is inherently gauge dependent. Later Feynman diagrams were used to calculate the potential in the Post-Newtonian (PN) approximation by using scattering amplitudes [6–8]. The idea was to utilize the relation between the quantum mechanical scattering amplitude and the Fourier transform of the potential ($\tilde{V}(\mathbf{q}^2)$) in the center of mass frame

$$M(\mathbf{p}_1, \mathbf{p}_3, m_i) = - \int dt \tilde{V}((\mathbf{q}^2, v_1, v_2)). \quad (1)$$

While certainly these results were very interesting from a formal point of view, past this point it was not clear if the non-geometric approach could bear much fruit, at least as far as classical GR is concerned. It does seem that this line of reasoning did not have much impact on the relativity community, perhaps because no new results were generated.

It is interesting to note that in his talk at this conference, Feynman bemoaned the lack of experimental results in relativity [3]. But it is exactly phenomenological questions regarding newly developed experiments that has recently brought these non-geometric ideas back to relevance. Gravitational wave detectors hold the promise to open new windows in astronomy and astro-physics by detecting the signatures of binary inspirals. The utility of these experiments is predicated on our ability to make precise predictions. Not surprisingly there has been a tremendous effort put into generating these predictions both analytically and numerically.³ Numerical techniques concentrate on the late stages of inspiral, which are (at least at this time) out of the reach of analytic techniques as, in this regime, there is no controlled approximation in which to work. Analytic calculations can be performed during early stages of infall when the constituents are well separated. Within this window there are two possible expansion parameters with which one can perform a well controlled approximation. For Extreme Mass Ratio Inspirals (EMRI) the ratio of masses $\tau \equiv (M_L/M_H) \ll 1$ determines how the background geometry traversed by the light mass deviates from Schwarzschild, i.e. this is the probe limit. While in the case of a small relative velocity v/c , we have the PN approximation in which the space-time is nearly Minkowskian. The former case is

² This term is perhaps too strong a statement, as geometry always plays a role. The word demi-geometric would probably be more appropriate.

³ It would appear to me, that the amount of effort going into analytic calculation has been dwarfed by the numerical effort especially within the United States. This is just the perception of an outsider and is completely anecdotal.

really semi-analytic as calculating Greens function in the Schwarzschild background entails numerical work.

In both the EMRI and PN cases the relevant physical observable is the wave form at null infinity. If we think of the binary system as a black box then clearly we should be organizing our calculation by considering the binary system as a single entity. In the case of EMRI we calculate the radiation of the small mass constituent moving in the Schwarzschild background while in the PN case the system can be considered a point like object endowed with a set of time dependent multipole moments. The calculational challenges in the two cases are quite distinct. In the EMRI problem one needs to utilize the nettlesome Schwarzschild propagator. Indeed, this is sufficiently challenging that even getting leading order results is no simple task. On the other hand the leading order PN calculations are essentially trivial, moreover, phenomenologically it is important to produce accurate wave forms in order to be able to do parameter estimation. Thus the challenge in the PN case is to be able to calculate systematically to as higher an order as possible.

In both cases we have problems with diverse scales. In the EMRI case we have only two relevant scales. The size of the smaller constituent (or the mass) and the curvature scale of the background. While for the PN case we have: the size of the constituents R_i , the radius of the system r and the wavelength of the radiation, which scales as r/v . The multi-scaled nature of these problema is what motivates the use of effective field theory (EFT).

EFT is a tool developed for quantum field theories. The fundamental ideas involved date back to the original work on the renormalization group where one utilizes the fact that short distance and long distance physics factorize as a consequence of the local nature of physical laws. That is to say, if we have an action (or Hamiltonian) which correctly describes the microscopic physics up to some scale Λ

$$H = \sum_i C_i O_i, \tag{2}$$

where O_i are some generic operators and C_i are a set of accompanying constants sometimes called “Wilson coefficients”. If we are interested in getting an approximate description of the theory at low energies ($E \ll \Lambda$) then we may utilize an effective Hamiltonian

$$H' = \sum_i C'_i O'_i. \tag{3}$$

In general H' is “simpler” than H . For instance in a QFT H will in general involve more particles species than H' . In principle the sum in (3) is infinite while the sum in (2) is finite.⁴ However, the sum is cut-off after one utilizes the fact that we can power count the operators in E/Λ . This is typically done by dimensional analysis, where

⁴ In the old days these two theories would be called “non-renormalizable” and “renormalizable” respectively.

any operator with mass dimensions⁵ d is suppressed by powers of $(E/\Lambda)^{(4-d)}$. In more general theories, such as will be discussed in a rest of this article, the operators will be power counted in some other expansion parameter such as v in the case of the PN expansion. The C' are determined, if the microscopic theory is not strongly interacting,⁶ by a matching procedure, in which one matches the value some object (which need not be physical) in the effective theory (3) to its full theory result. This matching procedure is often said to entail “integrating out the degrees of freedom between Λ and E ”. This seems to be an inherently quantum/statistical mechanical notion since it implies we are performing a path integrals over fluctuating degrees of freedom. However, the idea applies classically as well, in which case it simply means we are eliminating a field from the action by using its equation of motion and then expanding the propagator (in momentum space) to generate a local action.⁷ As a trivial example suppose we have an action for heavy field ϕ_H and light field ϕ_L given by

$$S = \int d^4x \left(\frac{1}{2}(\partial\phi_H^2) - \frac{1}{2}m_H^2\phi_H^2 + \frac{1}{2}(\partial\phi_L^2) - \lambda\phi_L^2\phi_H \right). \quad (4)$$

At energies and momenta much below m_H we may approximate $\phi_H \approx \lambda\phi_L^2/m_H^2$ leading to an effective theory with a self interaction $\lambda^2\phi_L^4/m_H^2$. This corresponds to performing a saddle point approximation for the ϕ_H path integral. In classical theories these masses would be replaced by some other scales such as typical sizes of macroscopic objects, or distance between objects. Finally we note that we can avoid calculating coefficients of operators⁸ which are forbidden by symmetries since they necessarily vanish. That is, we can write down the effective theory directly simply by including all possible operators allowed by the symmetries.

At first site it appears that integrating out the short distance modes does not buy you much, given that we are asking the user to calculate in the full theory which presumably we were trying to avoid in the first place. However, the choice of matching calculation is up to the practitioner. That is, one can choose to match anything which is well defined, even if it is gauge dependent, since the coefficients themselves are gauge invariant. Thus the full theory calculation that needs to be done is typically much simpler then any full theory calculation that one would be interested in performing should one choose not to use EFT. This will be clarified and exemplified below.

In the EFT the low energy theory only contains light degrees of freedom, but where is the pay off in this procedure? Technically, reducing the number of scales simplifies calculations in the low energy theory. In particular, a plurality of scales can lead to integrals which may not have closed form solutions. Moreover, working in the EFT allows one to sum logarithms of the form $\alpha \text{Log}(m_H/m_L)$ which may jeopardize the

⁵ Through out this article we will be using units. $c = \hbar = 1$.

⁶ This is the case in QCD when one tries of determine the dynamics of low energy Goldstone bosons (pions). In this case one has to fix the coefficients C'_i by using data.

⁷ It is not always true that one can expand the propagators, in which case the action becomes non-local. In the non-relativistic case (PN) this leads to an action which is non-local in space, while in the EMRI case it's non-local in time as well.

⁸ We use this term, much to the dismay of many a referee, even when dealing with classical theories.

utility of perturbation theory.⁹ Formally, this explicit mode separation (factorization), with the short distance modes being absorbed into the coefficients C_i , allows one to control the systematics. In the cases of classical EFT that will be discussed here, working in the EFT allows us to utilize techniques from the non-geometric approach to GR such as Feynman diagrams. Furthermore, working at the level of the action allows one to handle ultra-violet divergences, which inevitably arise in any EFT, even classically, as consequence of the fact that the EFT mutilates the UV physics, via standard renormalization techniques. In particle physics mode factorization allows one to calculate scattering cross sections between nucleons at high energies [9] which is of crucial importance for understanding the scattering of protons at the LHC.

2 The extreme mass ratio problem

From the EFT point of view the EMRI problem is formally rather simple. We first integrate out all of the modes which are responsible for the internal dynamics of the probe (small mass) constituent. The resulting EFT, valid at distance larger than the size of the object is nothing but the theory of a point particle. Following EFT reasoning we write down all terms consistent with the symmetries, which in this case are general coordinate invariance and world-line reparameterization invariance

$$S_{E+B} = \int d\tau (-m + C_E E_{\mu\nu} E^{\mu\nu} + C_B B_{\mu\nu} B^{\mu\nu} + \dots), \tag{5}$$

where the electric and magnetic Weyl tensors are defined as

$$E_{\rho\mu} = C_{\rho\sigma\mu\nu} v^\sigma v^\nu \tag{6}$$

$$B_{\alpha\mu} = \frac{1}{2} \star C_{\rho\sigma\mu\nu} v^\sigma v^\nu \tag{7}$$

with v being the world-line tangent vector. Notice that operators which vanish via the equations of motion have not been included, as they can be removed via a field redefinition and can thus not contribute to any physical quantity (for a discussion of this see [14]). The series (5) has been truncated as higher dimension terms are suppressed by powers of the size. Indeed, for a black hole coefficients $C_{E,B}$ scale as $M_{pl}^2 r_s^5$. These operators induce geodesic deviation and can be thought of as polarizabilities. In fact, C_E is related to the static tidal Love number. These matching coefficients are, in general, scale dependent. That is, when we calculate in this effective theory we will face UV divergent integrals which need to be regulated. When these divergences are logarithmic the regulator necessitates the introduction of a scale. It is easiest to regulate using dimensional regularization as it preserves the symmetries of the action.

⁹ In the case of classical EFT this is typically not true. For instance in the PN expansion every log is accompanied by factors of v . Thus while the logs may dominate the terms at some fixed order in v , re-summation does not improve the accuracy of the prediction.



Fig. 1 The diagram on the LHS is the leading order contribution to the effective action, while the diagram on the *right* is a correction due to bulk interactions

Once regulated the divergences can be absorbed into the matching coefficients, which induces the aforementioned scale dependence. It is exactly this scale dependence which allows for the resummation of logs, as discussed below.

At this point there are no further short distance scales to remove in the case of the EMRI. The only remaining relevant scale is the R ,

$$R \sim \sqrt{\frac{M_{pl}^2 r^3}{M_H}}. \quad (8)$$

We can then see that the expansion parameter r_0/R (where r_0 is the size of the smaller mass object) becomes M_L/M_H and at strong coupling $r = M_H/M_{pl}^2$.

One may now calculate the radiation by calculating the motion of the probe particle and convolving the resulting trajectory with a retarded Greens function, which is technically challenging. Even the leading order radiation is troublesome due to the lack of a closed form expression for the retarded propagator in the Schwarzschild background. Recent progress in this direction was made in Wardell et al. [16], Zenginoglu and Galley [17]. Beyond leading order in the mass ratio one has to include the self-force effects which are both dissipative as well as conservative in nature. The calculations of the self-force in the EFT were pioneered by Galley and his collaborators [18–20]. One calculates the effective action within the closed-time path formalism by calculating all diagram where there are no open graviton lines as shown in Fig. (1). One then varies this action with respect to the world-line to derive the self-force equation. Diagrams with higher order graviton vertices in the bulk are suppressed.

3 The Post-Newtonian case

In the PN case there is an additional hierarchy of scales. The relevant scales are now R , r and r/v corresponding to the typical size of the constituents, the radius of the orbit and the wavelength of the radiation, respectively. Thus once we have integrated out the scale $1/R$ we must now integrate out the scale r . The resulting theory will only have one relevant scale, vr . To achieve this goal we must determine the relevant modes in the theory. I will not go through the derivation here, but suffice it to say that the analysis very similar to the case of NRQCD, the theory of non-relativistic quarks. For a discussion of the mode analysis see [14]. The result is that the relevant regions of momentum space correspond to potential modes and radiation modes¹⁰ with

¹⁰ In the language of asymptotic expansions these correspond to the near and far fields.

momenta which scale as $p^\mu \sim (v/r, 1/r)$ and $p^\mu \sim (v/r, v/r)$ respectively. EFT's with these types mode decompositions are sometimes called "modal" to distinguish them from more canonical EFT's. The potential mode has a invariant mass which is large compared to the radiation mode and gets integrated out. This is accomplished by decomposing the graviton field into a potential (H) and radiation (h) modes

$$g_{\mu\nu} = \eta_{\mu\nu} + \frac{H_{\mu\nu}}{M_{pl}} + \frac{h_{\mu\nu}}{M_{pl}}. \tag{9}$$

In this procedure manifest diffeomorphism invariance is preserved by working in the background field gauge. That is, the long wavelength radiation mode is frozen while we integrate out the potential mode to generate an action for the radiation mode. To do this systematically, as an expansion in v , entails first deriving a set of power counting rules for the fields such that each term in the action $S(h, H)$ scales homogeneously in v . This forces us to perform a multipole expansion [15] at the level of the action, which will play an important role when we renormalize the theory. By having a manifest power counting for each term in the action we can determine which Feynman diagrams contribute at a given order in v .

Next one integrates out the potential mode by calculating all Feynman diagrams with no open potential lines.¹¹ We do however include diagrams with open radiation lines, as these will generate couplings in the low energy action between the potentials and the radiation (see Fig. (2)). Formally integrating out the potential modes can we written as

$$\int DhDH e^{iS(h,H)} = \int Dhe^{iS(V,O,h)} \tag{10}$$

where V are a set of potentials which depend upon the orbital radius and velocities, and O is a set of multipole moments (which are functions of the world lines of the constituents) for the coarsed grained binary, which is now treated as a point particle.

The calculation of potentials using this methodology can be automatized as was done by Foffa and Sturani [21] who calculate the 3PN potential, as well as pieces of the 4PN result [22]. By using Kaluza-Klein variables [23] one can reduce the number loops needed to calculate for odd power of n when working at $n - PN$, but even so, the number of diagrams grows as n -factorial. At the end of this article I will discuss ways of avoiding this problem. The full 4PN potential was recently calculated in Damour et al. [25] using more traditional methods. Three body, and beyond, potentials can be calculated simply by adding more world lines and keeping track of all the possible Feynman diagrams [13]. Finally, by power counting [10–12] the finite size operators (5) one concludes that these effects don't show up until $5PN$. This reproduces the so-called "effacement theorem" [24].

¹¹ These diagrams which be two particle irreducible to avoid double counting. That is, one should not be able to disconnect the diagram by cutting the two matter worldlines.

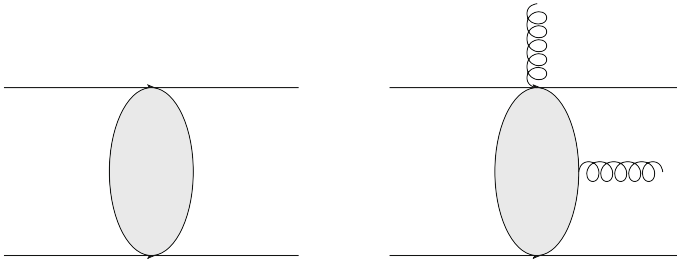


Fig. 2 On the *left* is a generic diagram that contribute to the potential. The blob corresponds to a collection of potential *graviton lines*. The diagram on the *right* represent the generic form which contributes to the coupling of the radiation field to the multipole moments

3.1 Spin

The introduction of a spin degree of freedom onto the world line was accomplished by Porto [26]. One introduces $S_{\mu\nu}(\tau)$ which is conjugate to the rotational frequency. The action is then written as a Routhian, i.e. a Hamiltonian/Lagrangian for the spin/worldline degrees of freedom

$$R = - \sum_i \left(M_i \sqrt{u_i^2} + \frac{1}{2} S_i^{ab} \omega_{ab\mu} u_i^\mu \right). \tag{11}$$

Given this action one generates a set of vertices in the action which can be used to build up Feynman diagrams for the potentials. ω is the spin connection and the small Roman letters represent the local orthogonal frame. The finite size effects for spin contribute at order 3PN. These can be calculated by including the the higher dimension operators analogous to (5)

$$L_{ES^2} = \frac{C_1}{2mM_{pl}} \frac{E_{ab}}{\sqrt{u^2}} S_c^a S^{cb}. \tag{12}$$

In addition there is a term that arises from necessitating that the spin supplementarity condition be preserved upon evolution

$$L_{RS^2} = - \frac{1}{2M} R_{deab} S^{cd} S^{ab} \frac{u^e u_c}{\sqrt{u^2}}. \tag{13}$$

Notice that the coefficient of the ladder term is fixed, while in the former C_1 depends upon the short distance physics and is given by $C_1 = 1$ for a spinning black hole. The 3PN potential proportional $S_1 S_2$ was calculated in Porto and Rothstein [27]. These results did not agree with the subsequent results calculated using more traditional methods (TM) in Steinhoff et al. [28]. This was shown [29,30] to be due to the fact that the results in Porto and Rothstein [27] did not include the contributions which carry over from the SSC effect in the lower order spin-orbit contribution. Once these terms were included the results did agree. The terms proportional to S_1^2 were calculated

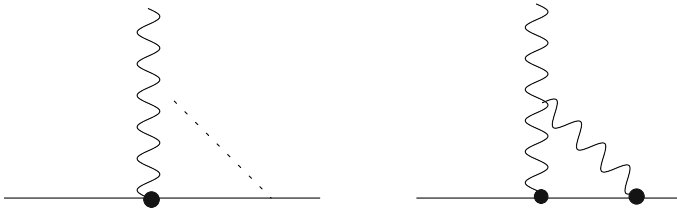


Fig. 3 On the *left* is the relevant diagram for the tail effects. The *dotted line* is a potential graviton, while the full *curly line* is a propagating radiation graviton. The diagrams on the *right* is the non-local in time memory effect. The heavy *black dots* represent the insertion of a time dependent moment

in Porto and Rothstein [31] and were corroborated in Steinhoff et al. [32]. The 4PN $S_1 S_2$ potential was calculating using EFT in Levi [34] and using TM in Steinhoff et al. [32]. Whether or not the results agree is not known at this time.

3.2 Radiation

The radiative moments arise from two sources in the low energy theory $L(O, h)$. The direct coupling of the radiation field to the matching coefficients (in this case being the moments O) and radiative moments which arise from the scattering of radiation off of the background geometry (tail effects) and or radiation (memory effects). These arise from the diagrams shown in Fig. (3), respectively. The moments O are calculated as matching coefficients when integrating out the potential modes. In the EFT methodology the higher order calculations were performed in the case of spinning constituents. All of the moments necessary to calculate the 3PN phase for spinning binaries and 2.5 amplitude were calculated in Porto et al. [35,36]. Figure (4) shows a set of non-linear contributions to the 3PN moments. When calculating the moments the external radiation graviton is truncated.

The procedure for calculating linear piece of the wave-from (i.e. ignoring bulk interaction) is canonical (see for instance [37]). To extract radiative moments, we start with the expression for the GW amplitude for a given stress energy source T^{ij}

$$h_{ij}^{TT}(t, \mathbf{x}) = -\frac{4G}{|\mathbf{x}|} \Lambda_{ij,kl} \int_{-\infty}^{+\infty} \frac{d\omega}{2\pi} T^{kl}(\omega, \omega \mathbf{n}) e^{i\omega t_{ret}} + O\left(1/|\mathbf{x}|^2\right). \quad (14)$$

where $\Lambda_{ij,kl}$ is the transverse traceless projector ant t_{ret} is the retarded time. We then calculate T_{ij} by calculating the one-point function $\langle h_{ij}(x, t) \rangle$, as in Fig. (4) truncating the external line. When calculating radiative moments, such as those in Fig. (3), IR divergence arises from integrating over the position of the three graviton vertex which can be arbitrarily far from the source since the potential generated from the mass only drops as $1/r$. These divergences can be resummed into the Coulomb phase, and are not of any physical significance as the IR divergence should be cut off by the finite time interval of the measurement. One needs to measure the phase at a point in time, to absorb the IR divergence. By matching the result to the form of the coupling to the

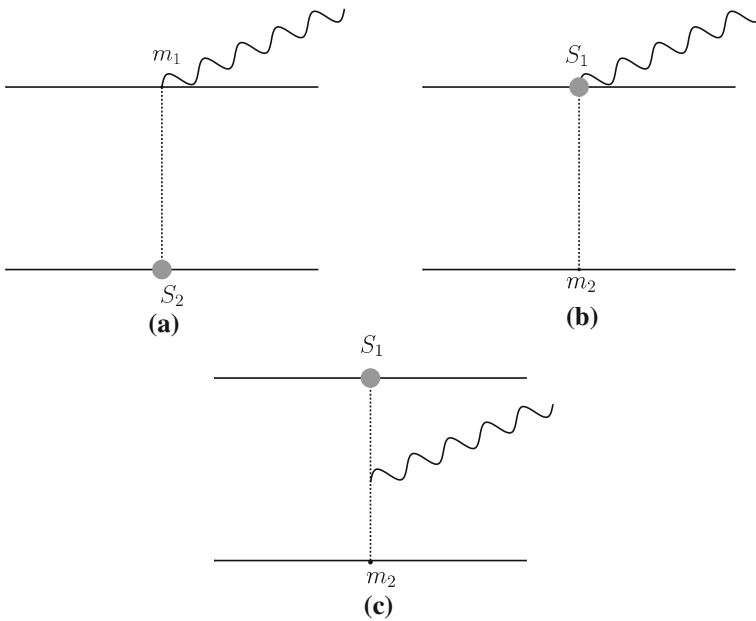


Fig. 4 First non-linear diagrams that contribute to the current (magnetic) octopole J^{ijk}

quadrupole moment one can extract the radiative moment

$$I_{rad}^{ij}(\omega) = I_0^{ij} \left(1 + GM\omega(\text{sign}(\omega)\pi + i \left[\frac{2}{\epsilon_{IR}} + \log \frac{\omega^2}{\mu^2} + \gamma_E - \frac{11}{6} \right] \right), \quad (15)$$

The arbitrariness in the scale μ reflects the arbitrary initial phase of the system.

3.3 Renormalization and summing logs

In the EFT formalism one also encounters UV divergences. Given that the full theory is UV finite, we know that these singularities are artifacts of our approximation scheme. Recall that we broke the EFT process into two steps. First we integrated out the modes which are responsible for the internal dynamics of the individual constituents. This led to a theory of point particles. The point particle limit can obviously be singular, and responsible for (some) sub-set of UV divergences. While in the second stage, where we integrate out the potential modes, leading to the theory of a point particle with dynamical moments, we expect to generate further UV divergences. In both case we know how to handle these divergences. Since UV divergences are always local they can be absorbed into “counter-terms” (i.e. coefficients of operators in the action). Since those coefficients, after renormalizaion, are fixed by a matching procedure there is no loss in predictive power. It is important to remember however, that not all UV divergences are equivalent. Power divergences can have no effect on any observable. The reason is that that they do no generate any non-analytic dependence on momenta.

Thus they are what’s known as “pure counter-term”, and can simply be discarded. Note that when we use dimensional regularization this happens automatically (e.g. $\int \frac{d^{4-2\epsilon}k}{k^2} = 0$). Logarithmic divergences, on the other hand, are always accompanied by $Log(p^2/\mu^2)$ which can not be absorbed into a counter-term. Furthermore, given that the result must be μ independent we know that the operator coefficients must depend upon μ in such a way as to make the result μ independent. This leads to the renormalization group (RG) equations equation, which, when solved, generate an infinite tower of logarithms for free. Using the RG equations Goldberger and Ross were able to sum an infinite set of logs which correct the quadrapole moment. The relevant UV divergence arises from diagrams such as the tail diagram shown on the LHS of (3) but with yet another potential graviton strung from the particle to the radiation, forming a four graviton vertex. The divergence arises when that vertex overlaps with the effective world line. The divergence is absorbed into the quadrapole. The resulting RG equation is given by

$$\mu \frac{d}{d\mu} Q = -\frac{214}{105} (Gm\omega)^2 Q \tag{16}$$

such that

$$Q(\omega, \mu) = (\mu/\mu_0)^{-214/105(Gm\omega)^2} Q(\omega, \mu_0) \tag{17}$$

This running corresponds to integrating out the modes between $\mu_0 = 1/r$ and $\mu = 1/(rv)$. Expanding this result for small v leads to a series of logs. In the test mass limit the results have been checked up to order $Log^3(v)$ and agreement has been found [39].

In addition to the quadrapole renormalization, the one body theory of moments also involves mass renormalization [40]. This renormalization arises from self energy diagrams involving one mass insertion and two quadrapole insertions. The log which arises is the classical equivalent of the “Bethe Log” which arises in the Lamb shift. The shift in the mass results in a non-local in time contribution to the Hamiltonian¹², as calculated in Damour et al. [25]. The resulting RG equation is given by

$$\mu \frac{d}{d\mu} \log \bar{m} = -2G^2 \langle Q_{ij}^{(3)} Q_{ij}^{(3)} \rangle (\mu), \tag{18}$$

where the brackets denote averages over a period. In the parlance of quantum field theory we would say that the mass “runs”, i.e. it is scale dependent. It is important to remember that this mass is scheme dependent (i.e. it depends upon the choice of counter-terms which has a finite ambiguity) and unphysical. It is only a place holder, i.e. it only shows up in intermediate stages of calculations of physical quantities which are scheme independent. However, using this renormalized perturbation theory allows us to calculate a set of logs which contribute to the energy [40]. One can expand the solution to this equation and generate logarithmic contributions to the energy. The 4PN log for a quasi circular orbit is found to agree with the results in Blanchet et al.

¹² I thank Gerhard Schaefer for conversations on this result.

[41]. Expanding out the mass to higher orders would generate an infinite tower of logs, but at any given order there are other sources of logs as well, coming from the higher renormalization of the multipole moments. So an additional calculation would have to be done to get the complete set of logs at a higher orders.

3.4 Finite size effects and dissipation

Let us now return to the finite size operators (5). These operators are the leading contributions to deviations from geodesic motion. As previously noted, they do not contribute until $5PN$, however, it's possible that for neutron stars they may be numerically enhanced. In any case formally they are still interesting as in principle they could also get logarithmically renormalized. Physically, these operators are generalized polarizabilities. However, if we are going to allow for deformations we should also allow for dissipation, as distorting the objects will naturally change their internal energy. Dissipation is notoriously difficult to handle at the level of a Lagrangian, which naturally leads to unitary (conservative) dynamics. To get around this issue we allow for new degrees of freedom [42,43] on the world line to absorb the internal energy ¹³ $Q_{ab}(\tau)$ whose coupling to the world line is uniquely fixed by symmetry

$$S_{dis} = \int d\tau (E_{ab} Q_{ab}(\tau) + B_{ab} Q_{ab}(\tau)). \tag{19}$$

$Q(\tau)$ is an operator which acts of on a Hilbert space representing some unknown degrees of freedom. This picture seems, at first glance, to be surrendering predictive power. Nonetheless, let us see how these terms in the action effect the potential between our constituents. The leading contribution to the potential arises from the box diagram shown in fig (3.4). The state of the system $|\Omega\rangle$ most likely is a mixed state which we might expect to be thermal (more on this below). Note that this diagram looks two particle irreducible, however, it is not since the intermediate lines are now dynamical, and not part of the iterative potential. The imaginary part of this diagram generates an absorptive potential. Note that the degrees of the freedom on the world line can not be gapped, otherwise the imaginary part of the $Q(\tau)Q(0)$ correlator would not have an imaginary part in the zero energy limit (Fig. 5).

Evaluating this diagram gives [42]

$$-iVT = \frac{M_2}{1024\pi^2 M_{pl}^4} \int d\tau d\tau' \langle \Omega | T(Q_1^{ij}(\tau) Q_1^{kl}(\tau')) | \Omega \rangle q_{ij} q_{kl} + (1 \leftrightarrow 2), \tag{20}$$

where $q_{ij} = \partial_i \partial_j \frac{1}{|\mathbf{x}_1 - \mathbf{x}_2|}$ and $|\Omega\rangle$ is the ground-state of the object. Now we use the fact that the imaginary part of the correlator is directly proportional to the graviton

¹³ For an alternative approach see [44], [45].

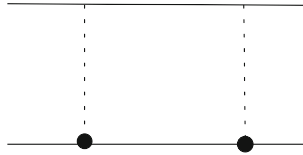


Fig. 5 The leading contribution to the dissipative potential. The blobs indicate an insertion of an operator of the form (19). The line between the blobs corresponds to the dynamical propagation of the underlying/unknown degrees of freedom

absorptive cross section, and thus we can write the differential power loss as

$$\frac{dP}{d\omega} = -\frac{1}{T} \frac{G}{64\pi^2} \sum_{a \neq b} \sigma_{abs}^b(\omega) M_a^2 |q_{ij}(\omega)|^2. \tag{21}$$

The power of this result is that it is universal. The dependence on the internal dynamics resides only in the absorptive cross section.

What about the real part of the correlator? In the limit of vanishing frequency the real part generates a local interaction. In fact, if we are considering the electric or magnetic quadruples then this limit of the real part will exactly mimic the contribution of the operators in (12).¹⁴ Remarkably, it has been shown by several groups that the coefficient a_R is zero for black holes [46–50]. In Chakrabarti et al. [49,50] this coefficient was calculated by solving the Regge Wheeler equation in the full theory and comparing it to the solution in the effective theory with a point particle source and a dynamical quadruple degree of freedom. The Fourier transformed of the correlator¹⁵ can then be read off from the linear response relation

$$Q^{ab}(\omega) = -\frac{1}{2} E_{BG}^{ab}(\omega) F(\omega). \tag{22}$$

Expanding this response function in small ω

$$F(\omega) \approx (a_R + ia_I + \omega(ib_I) + \omega^2(c_R + ic_I) + \dots) \tag{23}$$

By comparing to the full theory one may extract the coefficients it was found that $a_R = 0$ which in turn implies that $C_E = 0$. It was also found that c_R is non-zero and that it depends logarithmically on ω . That is, the Wilson coefficient for the operator $(\dot{E})^2$ is scale dependent. The matching for the magnetic piece has yet to be done to date.

¹⁴ Indeed we can choose to completely absorb the effect of these local operators in the correlation functions of the Q 's.

¹⁵ In linear response theory the relevant correlator is retarded. However, away from the poles the retarded and time ordered products are identical.

Note that the vanishing of a_R does not imply that the black hole does not have a DC (electric) susceptibility since there is still a non-zero response, as the Schwarzschild solution deforms. However, it does mean that if we assumed that the magnetic response also vanished, then there would be no geodesic deviation up to four derivatives. Indeed, given the lack of a symmetry argument that would pick out the spin two representation as being special, it is tempting to conjecture that *all* the static susceptibilities vanish. This would be quite remarkable. However given the singular (in the literary sense) nature of black holes it would not be a complete surprise.

Also note that C_E is gauge invariant despite the necessary choice of frames in doing the matching, so it is unambiguous. It is important to appreciate that these results do not mean that this coefficient does not get renormalized. Indeed in the effective theory one needs power law counter-terms. However, crucially this result implies that there are no logarithmic divergences. Thus the coupling does not run, if it's zero at one scale it's zero at all scales. Its vanishing however, is quite "unnatural" (for a discussion of naturalness in the context of QFT see [14]). This is a fine tuning problem, we would expect the coefficient to take a value on which scales with the UV cut-off (r_s), but instead it's zero, with no apparent symmetry to protect it. The unnaturalness is also manifest when considering [52] the spectral decomposition of the retarded correlator,¹⁶ we find that

$$\text{Re}F(\omega) = P \sum_m \frac{|\langle \Omega | Q_{ab} | m \rangle|^2}{E_\Omega - E_m - \omega}. \quad (24)$$

If we look at the DC response we are left with the rather remarkable result

$$\sum_m \frac{|\langle \Omega | Q_{ab} | m \rangle|^2}{E_\Omega - E_m} = 0. \quad (25)$$

which seems to imply that the state $|\Omega\rangle$ can not be pure given the the denominator has a fixed sign. Suppose that the state $|\Omega\rangle$ is thermal then we find

$$\sum_{m,n} e^{-\beta(E_n)} \frac{\langle n | Q_{ab} | m \rangle \langle m | Q_{ab} | n \rangle}{E_n - E_m} = 0, \quad (26)$$

which would imply a delicate cancellation. It is interesting to note that a similar effect arises in the theory of dissipative fluids [51]. Given the membrane paradigm the possible connection is quite tantalizing.

3.5 Further De-Geometrization

Finally I would like to come back to the topic introduced at the beginning of the talk. We have seen that thinking about GR as a gauge theory, much like QCD, has some calculational benefits. However, we have not really fully de-geometrized the problem.

¹⁶ The time ordered product and the retarded correlator differ only in their treatment of the poles.

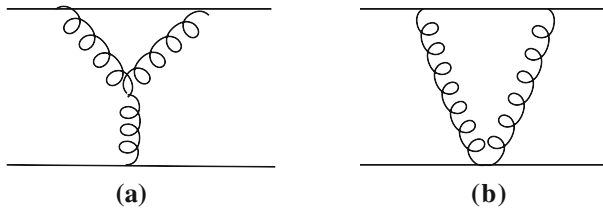


Fig. 6 One loop diagrams which contribute to the 1PN potential

We still needed to rely on the Einstein-Hilbert action to generate a set of Feynman rules. A completely geometric approach should not depend upon an action which followed from the principles of GR. Furthermore, we have also seen that calculating Feynman diagrams when going to higher orders can be quite cumbersome. As previously discussed the number of diagrams grows factorially with the order of the calculation. Moreover, as one goes to order n one needs to include the interactions which have $n + 1$ gravitons, which becomes rapidly computationally intensive.

In fact the proliferation of Feynman diagrams is a direct result of the fact that the Einstein-Hilbert action carries with it gauge redundancies which are forced upon us by general coordinate invariance. Modern amplitude techniques [53] have taught us that calculating Feynman diagrams is a highly inefficient way to proceed. The reason being that individual diagrams are not gauge invariant and as a consequence all the extra baggage associated with the unphysical degrees of freedom need to be kept. If, on the other hand, we concentrate on calculating physical quantities things simplify greatly. Indeed when calculating on-shell scattering amplitudes, we only need the (on-shell¹⁷) three graviton amplitude as all the higher point scattering amplitude can be fixed using the BCFW recursion relations [54,55]. Moreover, the three graviton amplitude can be fixed by Lorentz covariance [56]. So if we are only interested in calculating on-shell quantities all of the non-linearities inherent in the Einstein-Hilbert action are completely unnecessary. In a sense we can avoid Einstein formulation of GR completely. All on-shell scattering amplitudes can be fixed starting only with the assumptions of: Lorentz invariance, the existence of a massless spin-two particle and that the only poles in tree level amplitudes arise from particle exchange (this is a restatement of the locality assumption which goes into the BCFW recursion relations.). Most importantly, there is no need for Feynman diagrams since we use the aforementioned recursion relations. If one uses spinor-helicity notation the results for the full diagrams are quite compact.

This line of reasoning begs the question, what do on-shell quantities have to do with the potential, which is an inherently off-shell object? The answer resides in (1). If we can calculate the on-shell scattering amplitude, say between scalars, then we can extract the potential. However, as I mentioned above the on-shell construction of the n -point amplitude applies only to tree level diagrams while the potentials (beyond Newtons' law) arise from loop diagrams such as the ones shown in Fig. (6). Nonetheless, one can

¹⁷ Naively this amplitude is zero, however, if an external momentum is complexified this is not longer true. This complexification is necessary for the BCFW construction of recursion relations for the n -point on-shell S matrix element.

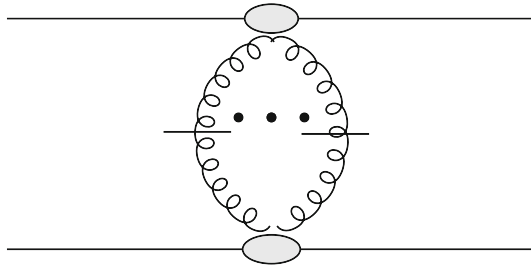


Fig. 7 Reconstructing the full scalar-scalar S-matrix by sewing together the scalar-scalar n point on shell scattering amplitudes. The *horizontal lines* represent the cuts which are lifted to allow the lines to be off-shell. The blobs represent a sum over all Feynman diagrams. A calculation which is avoided using the BCFW recursion relations

construct these diagrams from a pair of on-shell scalar-graviton n -point amplitudes using unitarity-sewing methods [57, 58] whereby the loop diagrams are constructed by sewing together two on-shell amplitudes and removing the on-shell conditions for the intermediate states. A generic potential generated in this way is shown in Fig. (7). Once the cut is lifted this generates the full scattering amplitude. Of course this includes quantum corrections, but it is simple to extract the classical pieces by looking at the form of the scalar integral. The final potential can be extracted after subtracting the iterations of lower order potentials. This procedure is demonstrated in Neill and Rothstein [59] where the 1-PN potential is calculated. In this paper it was also pointed out that using this technique one can generate solutions to Einstein's equation directly without ever writing down the equations themselves. That is, one can generate classical space-times directly from the S-matrix elements of massless spin two particles. This is done by calculating the potentials and taking the probe limit, i.e. where one of the masses goes to zero. The metric can then be extracted or by order in G_N by formulating the most general ansatz and fixing the coefficients via a matching procedure. Of course this technique is limited as it assumes asymptotic flatness. Nevertheless it is quite remarkable that classical space times emerge naturally from S-matrices with the only assumptions being: The existence of a massless spin two particle, Lorentz invariance and locality. It would be interesting to determine if this procedure can be generalized.

3.6 Conclusions

The EFT formalism has led to considerable progress in a relatively short period of time. In several areas the EFT formalism has matched the state of the art and in some cases, in particular calculations involving spin, exceeded it. Of course the long term impact of the program remains to be seen. I should also mention that the type of world line effective theory discussed here has been utilized in other contexts as well including: The calculation of black hole solutions in compact space-times [66–68], finite size effects in radiation reaction [64, 65], fluctuation forces on soft membranes [60–63], and Casimir forces between cogs [69].

Acknowledgments I would like to thank the organizers of GR20-Amaldi10 for the invitation to speak and for their gracious hospitality. I would also like to thank my collaborators on this subject, Walter Goldberger and Rafael Porto.

References

1. Gupta, S.N.: Phys. Rev. **96**, 1683 (1954)
2. Kraichnan, R.: Phys. Rev. **98**, 1118 (1955)
3. Feynman, R.P.: In: Brian Hatfield (ed.) Feynman Lectures on Gravitation. Addison-Wesley (1995)
4. Weinberg, S.: Phys. Rev. **135**, B1049 (1964)
5. Duff, M.J.: Phys. Rev. D. **7**, 2317 (1973)
6. Hiida, K., Okamura, H.: Prog. Theor. Phys. **47**, 1743 (1972)
7. Iwasaki, Y.: Prog. Theor. Phys. **46**, 1587 (1971)
8. Iwasaki, Y.: Lett Nuovo Cim **1S2**, 783 (1971)
9. Bauer, C.W., Fleming, S., Pirjol, D., Rothstein, I.Z., Stewart, I.W.: Phys. Rev. D. **66**, 014017 (2002). [[hep-ph/0202088](#)]
10. Goldberger, W., Rothstein, I.: Phys. Rev. D. **73**, 104029 (2006)
11. Goldberger, W.D., Rothstein, I.Z.: Gen. Relativ. Gravit. **38**, 1537 (2006)
12. [Int. J. Mod. Phys. D **15**, 2293 (2006)] For reviews see W. D. Goldberger, [hep-ph/0701129](#), and, S. Foffa and R. Sturani, [arXiv:1309.3474](#) [gr-qc]
13. Chu, Y.-Z.: Phys. Rev. D. **79**, 044031 (2009). [[arXiv:0812.0012](#)] [gr-qc]
14. Rothstein, I.Z.: TASI lectures on effective field theories. [arXiv:hep-ph/0308266](#)
15. Grinstein, B., Rothstein, I.Z.: Phys. Rev. D. **57**, 78 (1998). [[hep-ph/9703298](#)]
16. Wardell, B., Galley, C. R., Zenginoglu, A., Casals, M., Dolan, S. R., Ottewill, A.C.: [arXiv:1401.1506](#) [gr-qc]
17. Zenginoglu, A., Galley, C.R.: Phys. Rev. D. **86**, 064030 (2012). [[arXiv:1206.1109](#)] [gr-qc]
18. Galley, C.R., Hu, B.L.: Phys. Rev. D. **79**, 064002 (2009). [[arXiv:0801.0900](#)] [gr-qc]
19. Galley, C.R., Tiglio, C.R.: Phys. Rev. D. **79**, 124027 (2009). [[arXiv:0903.1122](#)] [gr-qc]
20. Birnholtz, O., Hadar, S., Kol, B.: Phys. Rev. D. **88**, 104037 (2013). [[arXiv:1305.6930](#)] [hep-th]
21. Foffa, S., Sturani, R.: Phys. Rev. D. **84**, 044031 (2011). [[arXiv:1104.1122](#)] [gr-qc]
22. Foffa, S., Sturani, R.: Phys. Rev. D. **87**(6), 064011 (2013). [[arXiv:1206.7087](#)] [gr-qc]
23. Kol, B., Smolkin, M.: Phys. Rev. D. **77**, 064033 (2008). [[arXiv:0712.2822](#)] [hep-th]
24. Damour, T.: The problem of motion in Newtonian and Einsteinian gravity. In Hawking, S.W., Israel, W. (eds.) Three Hundred Years of Gravitation, pp. 128–198. Cambridge University Press, Cambridge, New York (1987)
25. Damour, T., Jaranowski, P., Schafer, G.: [arXiv:1401.4548](#) [gr-qc]
26. Porto, R.A.: Phys. Rev. D. **73**, 104031 (2006)
27. Porto, R.A., Rothstein, I.Z.: Phys. Rev. Lett. **97**, 021101 (2006). [gr-qc/0604099]
28. Steinhoff, J., Hergt, S., Schaefer, G.: Phys. Rev. D. **77**, 081501 (2008). [[arXiv:0712.1716](#)] [gr-qc]
29. Porto, R. A., Rothstein, I. Z.: [arXiv:0712.2032](#) [gr-qc]
30. Porto, R.A., Rothstein, I.Z.: Phys. Rev. D. **78**, 044012 (2008). [Erratum-ibid. D **81**, 029904 (2010)] [[arXiv:0802.0720](#)] [gr-qc]
31. Porto, R.A., Rothstein, I.Z.: Phys. Rev. D. **78**, 044013 (2008). [Erratum-ibid. D **81**, 029905 (2010)] [[arXiv:0804.0260](#)] [gr-qc]
32. Steinhoff, J., Hergt, S., Schaefer, G.: Phys. Rev. D. **78**, 101503 (2008). [[arXiv:0809.2200](#)] [gr-qc]
33. Hartung, J., Steinhoff, J.: Annalen Phys. **523**, 919 (2011). [[arXiv:1107.4294](#)] [gr-qc]
34. Levi, M.: Phys. Rev. D. **85**, 064043 (2012). [[arXiv:1107.4322](#)] [gr-qc]
35. Porto, R.A., Ross, A., Rothstein, I.Z.: JCAP **1103**, 009 (2011). [[arXiv:1007.1312](#)] [gr-qc]
36. Porto, R.A., Ross, A., Rothstein, I.Z.: JCAP **1209**, 028 (2012). [[arXiv:1203.2962](#)] [gr-qc]
37. Thorne, K.: Rev. Mod. Phys. **52**, 299 (1980)
38. Goldberger, W.D., Ross, A.: Phys. Rev. D. **81**, 124015 (2010). [[arXiv:0912.4254](#)] [gr-qc]
39. Fujita, R.: Prog. Theor. Phys. **128**, 971 (2012). [[arXiv:1211.5535](#)] [gr-qc]
40. Goldberger, W. D., Ross, A., Rothstein, I. Z.: [arXiv:1211.6095](#) [hep-th]
41. Blanchet, L., Detweiler, S.L., Le Tiec, A., Whiting, B.F.: Phys. Rev. D. **81**, 084033 (2010). [[arXiv:1002.0726](#)] [gr-qc]
42. Goldberger, W.D., Rothstein, I.Z.: Phys. Rev. D. **73**, 104030 (2006). [[hep-th/0511133](#)]

43. Porto, R.A.: Phys. Rev. D. **77**, 064026 (2008). [[arXiv:0710.5150](#) [hep-th]]
44. Galley, C.R.: Phys. Rev. Lett. **110**(17), 174301 (2013). [[arXiv:1210.2745](#) [gr-qc]]
45. Grozdanov, S., Polonyi, J.: [arXiv:1305.3670](#) [hep-th]
46. Damour, T., Nagar, A.: Phys. Rev. D. **80**, 084035 (2009). [[arXiv:0906.0096](#) [gr-qc]]
47. Binnington, T., Poisson, E.: Phys. Rev. D. **80**, 084018 (2009). [[arXiv:0906.1366](#) [gr-qc]]
48. Kol, B., Smolkin, M.: JHEP **1202**, 010 (2012). [[arXiv:1110.3764](#) [hep-th]]
49. Chakrabarti, S., Delsate, Tr., Steinhoff, J.: Phys. Rev. D. **88**, 084038 (2013). [[arXiv:1306.5820](#) [gr-qc]]
50. Chakrabarti, S., Delsate, Tr., Steinhoff, J.: [arXiv:1304.2228](#) [gr-qc]
51. Endlich, S., Nicolis, A., Porto, R.A., Wang, J.: Phys. Rev. D. **88**, 105001 (2013). [[arXiv:1211.6461](#) [hep-th]]
52. Goldberger, W., Rothstein, I.Z.: unpublished work
53. For a review and references see, Bern, Z., Dixon, L. J., Kosower, D. A.: Annals Phys. 322, 1587 (2007) [[arXiv:0704.2798](#) [hep-ph]]
54. Britto, R., Cachazo, F., Feng, B.: Nucl. Phys. B. **715**, 499 (2005). [[hep-th/0412308](#)]
55. Britto, R., Cachazo, F., Feng, B., Witten, E.: Phys. Rev. Lett. **94**, 181602 (2005). [[hep-th/0501052](#)]
56. Benincasa, P., Cachazo, F.: [arXiv:0705.4305](#) [hep-th]
57. Bern, Z., Dixon, L.J., Dunbar, D.C., Kosower, D.A.: Nucl. Phys. B. **425**, 217 (1994). [[hep-ph/9403226](#)]
58. Bern, Z., Dixon, L.J., Dunbar, D.C., Kosower, D.A.: Nucl. Phys. B. **435**, 59 (1995). [[hep-ph/9409265](#)]
59. Neill, D., Rothstein, I.Z.: Nucl. Phys. B. **877**, 177 (2013). [[arXiv:1304.7263](#) [hep-th]]
60. Yolcu, C., Rothstein, I.Z., Deserno, M.: Euro. Phys. Lett. **96**, 20003 (2011)
61. Yolcu, Cem, Rothstein, Ira Z., Deserno, Markus: Phys. Rev. E. **85**, 011140 (2012)
62. Yolcu, C., Deserno, M.: Phys. Rev. **E86**, 031906 (2012)
63. Rothstein, I.Z.: Nucl. Phys. B. **862**, 576 (2012). [[arXiv:1111.0533](#) [hep-th]]
64. Galley, C.R., Leibovich, A.K., Rothstein, I.Z.: Phys. Rev. Lett. **105**, 094802 (2010). [[arXiv:1005.2617](#) [gr-qc]]
65. Galley, C.R., Leibovich, A.K., Rothstein, I.Z.: Phys. Rev. Lett. **109**, 029502 (2012). [[arXiv:1206.4773](#) [gr-qc]]
66. Chu, Y.-Z., Goldberger, W.D., Rothstein, I.Z.: JHEP **0603**, 013 (2006). [[hep-th/0602016](#)]
67. Chu, Y.-Z., Goldberger, W.D., Rothstein, I.Z.: JHEP **0909**, 104 (2009). [[arXiv:0908.3490](#) [hep-th]]
68. Chu, Y.-Z., Goldberger, W.D., Rothstein, I.Z.: Phys. Rev. D. **77**, 064033 (2008). [[arXiv:0712.2822](#) [hep-th]]
69. Vaidya, V.: [arXiv:1304.7475](#) [quant-ph]